N-terminal acetylation of the influenza ribonuclease PA-X promotes nuclear localization and host shutoff activity in a multifaceted manner

Raecliffe E. Daly[1,2], Idalia Myasnikov[2], Marta Maria Gaglia[2]

[1] Program in Cellular, Molecular and Developmental Biology, Tufts University Graduate School of Biomedical Sciences, Boston, MA, 02111, United States.

[2] Institute for Molecular Virology and Department of Medical Microbiology and Immunology, University of Wisconsin – Madison, Madison WI

Correspondence: marta.gaglia@wisc.edu

Abstract

To counteract host antiviral responses, influenza A virus triggers a global reduction of cellular gene expression, a process termed “host shutoff.” A key effector of influenza A virus host shutoff is the viral endoribonuclease PA-X, which degrades host mRNAs. While many of the molecular determinants of PA-X activity remain unknown, a previous study identified a requirement for N-terminal acetylation of PA-X for its host shutoff activity, but did not address how this modification promotes activity. Here, we report that PA-X N-terminal acetylation has two functions that can be separated based on the position of the acetylation, on the first amino acid, i.e. the initiator methionine, vs. the second amino acid following initiator methionine excision. Modification at either site is sufficient to ensure correct PA-X localization to the nucleus. However, modification at the second amino acid is not sufficient for host shutoff activity of ectopically expressed PA-X, which requires N-terminal acetylation of the initiator methionine specifically. Interestingly, during infection, N-terminal acetylation of PA-X at any position results in PA-X host shutoff activity, and this is, in part, due to a functional interaction with the influenza protein NS1. This reveals an unexpected role for other viral proteins in PA-X activity. Our studies highlight the multifaceted nature of PA-X N-terminal acetylation in its ability to regulate the host shutoff activity of PA-X through multiple avenues.

Introduction

Although influenza A viruses have a relatively small genome of around 13.5 kb in size, multiple influenza proteins are involved in modulating the host immune response. Of the influenza immunomodulatory proteins that have been identified to date, PA-X has emerged as a key factor in regulating gene expression and innate immune responses and is the major contributor to host shutoff, i.e. the global reduction of gene expression during influenza A virus infection[1–3]. Moreover, infection with viruses engineered to lack PA-X results in a stronger innate immune response and increased *in vivo* compared to WT influenza A virus infection[2,4]. Thus, PA-X limits the innate immune response during infection, which, in turn, reduces inflammation-induced pathology that ultimately leads to reduced mortality *in vivo.*

The reduction in the innate immune response and host shutoff are the result of the endoribonucleolytic (RNase) activity of PA-X[2,3,5]. To carry out host shutoff, PA-X degrades RNA polymerase II transcripts, while sparing RNAs generated from other polymerases, including the influenza RNA-dependent RNA polymerase generated viral RNAs[3,5]. While the host shutoff activity of PA-X is well established, limited information has been uncovered to date on how PA-X functions. In particular, whether and how PA-X activity is modulated in cells remains unclear.

A study by Oishi et al. in 2018 reported that during protein synthesis, PA-X is N-terminally acetylated by the host N-terminal acetyltransferase complex B (NatB). This co-translational modification is required for the host shutoff activity of PA-X[6]. N-terminal acetylation is a highly abundant protein modification in cells, with 80-90% of the human proteome acquiring this modification during protein biosynthesis[7–10]. It is catalyzed by several Nat complexes (NatA-NatF), which differ from each other based on their subunit composition and their substrate specificity profiles[11,12]. The substrate specificity is mainly determined by the first two N-terminal residues of the protein to be modified (Figure 1A)[11]. NatA, NatB, and NatC are responsible for

the majority of N-terminal acetylation events in eukaryotes[12]. NatB and NatC acetylate nascent polypeptides on the initiator methionine, while NatA modifications occur following the excision of the initiator methionine by host methionine aminopeptidases. Despite the fact that N-terminal acetylation is a common modification, only a handful of studies have investigated the effect of N-terminal acetylation on protein function[12,13]. Nonetheless, they have found multiple roles for this modification. N-terminal acetylation has been implicated in the control of protein stability[14–18], protein folding[19–21], protein-protein interactions[22–27], and subcellular targeting[28–31]. While PA-X requires this modification to function, it remains unknown how N-terminal acetylation supports PA-X host shutoff activity.

A complication in studying PA-X N-terminal acetylation is that PA-X shares its N terminus with polymerase acidic (PA), a subunit of the influenza RNA polymerase that is necessary for viral replication[2,32]. This is because PA-X is generated as an additional low abundance protein through ribosomal frameshifting after translation of the 191st amino acid of segment 3, which encodes PA[2,32]. Therefore, mutations or acetylase knockdown/outs that alter PA-X N-terminal acetylation also impact PA N-terminal acetylation, and PA also appears to require this modification for its function[6]. Due to this complication, the impact of PA-X N-terminal acetylation during infection was not separated from that of PA modification in the initial study.

Here, we report that N-terminal acetylation supports PA-X activity by two separate mechanisms. N-terminal acetylation is needed for the localization of PA-X to the nucleus. We and others have previously shown that nuclear localization is required for the host shutoff activity of PA-X[3,33,34]. Interestingly, we found that PA-X localizes to the nucleus when modified by Nat complexes that add the modification to either the initiator methionine or the second residue after the initiator methionine excision. However, in the absence of viral infection, the localization alone is not enough to confer host shutoff activity, and PA-X requires the modification specifically at the

initiator methionine to downregulate RNA levels in cells. This result suggests that the modification on the initiator methionine has a separate role in supporting PA-X host shutoff activity. To our surprise, we also observed that PA-X mutants that are modified at second amino residue are able to downregulate transcripts during infection, despite the fact that they are largely inactive when PA-X is ectopically expression. This discrepancy between ectopic expression and infection led us to discover that the viral protein NS1 promotes the host shutoff activity of PA-X. NS1 appears to promote RNA downregulation by PA-X mutants with low activity, suggesting that NS1 and PA-X proteins functionally interact in PA-X-driven host shutoff, as also recently suggested by Bougon et al.[35].

Results

N-terminal acetylation is required for the nuclear localization of PA-X and is also needed for additional functions

Previous studies using the influenza A/WSN/33 H1N1 (WSN) virus have shown that N-terminal acetylation of PA-X by the NatB complex is important for its host shutoff activity in mammalian cells[6]. When the N terminus of PA-X is mutated from ME- to MP- to produce non-acetylated PA-X proteins (Fig. 1A)[12,36], the shutoff activity of PA-X is lost[6]. While the functions of N-terminal acetylation have only been described in a handful of studies[14–31], one of the established functions of this modification is control of subcellular localization[28–31]. We and others have reported that PA-X must localize to the nucleus to downregulate mRNA[3,33,34]. To determine whether non-acetylated mutants lost activity because of incorrect subcellular localization, we compared the subcellular localization of ectopically expressed eGFP-tagged wild-type (WT) PA-X from the influenza A/Puerto Rico/8/1934 H1N1 virus (PR8) and the non-acetylated PR8 PA-X E2P mutant using confocal microscopy. To confirm that the PR8 PA-X E2P mutant lost activity, similarly to the WSN PA-X E2P mutant, we co-transfected cells with PA-X and a luciferase

reporter and measured luciferase RNA levels by qPCR, as we have done in previous studies[3,5]. As expected, the PA-X E2P mutant had no host shutoff activity, and luciferase levels in PA-X E2P transfected cells were similar to those in cells transfected with the catalytically inactive PA-X D108A mutant (Fig. 1B)[3,5]. To quantify PA-X localization unbiasedly, we computed Manders' overlap coefficients between the PA-X-eGFP signal and Hoechst nuclear staining from confocal microscopy images using the ImageJ plugin Just Another Colocalization Plugin (JACoP)[37]. Manders' overlap coefficient values range from 0 to 1. 0 indicates no overlap between the two signals and primarily cytoplasmic localization, whereas 1 indicates complete overlap and primarily nuclear localization. eGFP alone showed an average Manders' overlap coefficient of 0.52, indicating diffuse localization throughout the cells, and WT PA-X was predominantly nuclear, with an average Manders' overlap coefficient of 0.86, consistent with previous studies[3,33,34]. Interestingly, PA-X E2P was more diffusely localized than WT PA-X, and had an average Manders' overlap coefficient of 0.51, similar to eGFP (Fig. 1C, D). These results suggest that N-terminal acetylation is required for the nuclear accumulation of PA-X, which in turn could explain its loss of activity. As a control we also generated two mutants that have a different sequence but should still be modified by NatB, PA-X E2D and PA-X E2N (Fig. 1A). The NatB modified mutants PA-X E2D and PA-X E2N had a similar localization to WT PA-X (Manders' overlap coefficients = 0.88 and 0.86, respectively, Fig. 1F,G), as well as comparable host shutoff activity to WT PA-X (Fig. 1E). These results suggest that the differences seen between WT PA-X and PA-X E2P are due to changes in N-terminal acetylation, and not changes in the protein sequence.

To determine whether the decreased activity of PA-X E2P was due only to its incorrect subcellular localization, we fused PA-X E2P to the canonical SV40 nuclear localization signal[38] (PA-X E2P-NLS-eGFP). We found that, as expected, nuclear localization was restored for the PA-X E2P-NLS protein (data not shown). However, this mutant was still unable to downregulate

luciferase mRNA levels (Fig. 1B). This result indicates that nuclear localization alone is not enough to restore the host shutoff activity of unmodified PA-X. Therefore, to downregulate RNA levels in cells, PA-X also requires N-terminal acetylation for a second function.

General N-terminal acetylation is sufficient for PA-X localization to the nucleus, but not for activity

To further explore the relationship between the PA-X N-terminal acetylation, nuclear localization and host shutoff activity, we tested PA-X mutants that are modified by the host complex NatA. Unlike NatB-modified proteins, which are N-terminally acetylated at the initiator methionine, NatA-modified proteins are N-terminally acetylated at the second residue following methionine excision by host methionine aminopeptidases[12,39,40](Fig. 1A). A previous study showed that, like the non-acetylated WSN PA-X E2P mutant, the NatA-modified WSN PA-X E2A mutant loses its host shutoff activity[6]. We confirmed that this was also the case with the PR8 PA-X E2A mutant (Fig. 2A). In addition, we generated two additional NatA modified mutants, PA-X E2S and PA-X E2V, which also had no apparent host shutoff activity in cells (Fig. 2A). Interestingly, we saw that PA-X E2A and E2S had a similar localization to WT PA-X, and primarily accumulated in the nucleus (Fig. 2B,C). In contrast, PA-X E2V was more diffusely localized between the nucleus and the cytoplasm, similar to the unmodified PA-X E2P (Fig. 1C,D; Fig. 2B,C). For PA-X E2V, this decrease in nuclear localization could be due to the lower levels of N-terminal acetylation reported for proteins that start with MV-[9,40]. Taken together, these data suggest that N-terminal acetylation at high levels is sufficient for PA-X nuclear localization, but that this modification alone is not able to support host shutoff activity.

N-terminal acetylation at the initiator methionine promotes PA-X host shutoff activity

It is surprising that mutants that are still acetylated[6] and localized to the correct cellular compartment are inactive. The previous study hypothesized that perhaps the NatB complex activity, rather than the modification, was important[6]. However, NatA- and NatB-modified proteins also differ in the presence (NatB-modified) or absence (NatA-modified) of the initiator methionine and thus the location of the modification. To test if the site of the modification was the determining factor, we investigated the effect of modification by NatC, which also modifies proteins on the initiator methionine[9,12]. To do so, we employed two mutants that should be modified by NatC[9,12], PA-X E2M and PA-X E2L (Fig. 1A). The subcellular localization of the NatC-modified mutants was similar to that of WT PA-X (Fig. 3B,C). In addition, the NatC-modified mutants were also able to downregulate luciferase mRNA levels in cells, though to a lesser degree than WT PA-X and the other NatB-modified mutants (Fig. 3A). Thus, N-terminal acetylation of the initiator methionine is specifically required for the host shutoff activity of PA-X.

N-terminal acetylation by various Nat complexes has similar consequences on PA-X activity regardless of strain

While results with WSN[6] and PR8 PA-X are suggestive of a broader phenomenon, both of these strains are lab-adapted viruses. Therefore, we wanted to ensure that the phenotype of N-terminal acetylation mutants was also conserved with PA-X proteins from more relevant human seasonal influenza viruses. Currently circulating seasonal human viruses are H1N1 strains related to the pandemic 2009 H1N1 virus (H1N1pdm09), and H3N2 strains[41]. Thus, we tested the effect of E2P (no modification), E2A (modification by NatA), and E2M (modification by NatC) mutations in the PA-X sequences from A/Tennessee/1-560/09 H1N1 (H1N1pdm09) and A/Perth/16/2009 H3N2 (Perth). We found that the trend in host shutoff activity was similar among PA-Xs from all influenza A strains tested. All PA-X E2A and PA-X E2P mutants had significantly lower host shutoff activity, while the PA-X E2M mutants maintained an intermediate

amount of activity (Fig. 4). These data suggest that regardless of strain, PA-X requires N-terminal acetylation to access the nucleus and N-terminal acetylation of the initiator methionine specifically to downregulate RNA levels.

General N-terminal acetylation is sufficient for the host shutoff activity of PA-X during infection

Our results point to the importance of PA-X N-terminal acetylation for nuclear localization and host shutoff activity when PA-X is ectopically expressed in cells. However, we wanted to confirm that this modification also had a role during viral infection. This was not done in the previous study because of the challenge in separating PA and PA-X translation during infection, as PA-X is produced by a +1 frameshifting event that occurs after translation of the 191st amino acid of PA. Any mutation in the PA-X N terminus will also be present in PA because their N termini are identical[2], and PA also requires N-terminal acetylation for polymerase activity[33]. Thus, to separate PA and PA-X production, we examined the activity of ectopically expressed PA-X mutants in cells infected with a PA-X-deficient PR8 (PR8 PA(ΔX))[5]. We first transfected 293T cells with plasmids encoding eGFP, WT PA-X or the PA-X E2 mutants E2P (unmodified), E2D (NatB-modified), E2A (NatA-modified), and E2M (NatC-modified). We then either left cells uninfected or infected them with PR8 PA(ΔX) virus (Fig. 5). To test whether infection following transfection was successful, we measured HA RNA levels across all conditions. We found that transfecting cells did not prevent them from being infected with WT PR8 or PR8 PA(ΔX) viruses (Fig. 5A). To make sure that transfecting did not inhibit the ability of PA-X to downregulate its endogenous targets, we confirmed that G6PD is downregulated in WT infected cells (Fig. 5B). We then measured RNA levels of a co-transfected luciferase reporter to assess the activity of the mutants during infection. As expected, unmodified PA-X E2P remained inactive during infection, and NatB-modified PA-X E2D maintained host shutoff activity that was comparable to

WT PA-X (Fig. 5C). To our surprise, NatC-modified PA-X E2M and NatA-modified E2A had higher levels of host shutoff activity in infected vs. uninfected cells (Fig. 5C). These results suggest that there are additional factors during infection that enhance the host shutoff activity of PA-X mutants with attenuated host shutoff activity.

The influenza A virus protein NS1 potentiates PA-X activity during infection

A possible reason for the increased host shutoff activity of PA-X E2A during infection is a functional interaction between PA-X and another viral protein, even though this interaction is not strictly required for activity, based on ectopic expression experiments. To test this hypothesis, we compared mRNA downregulation by ectopically expressed WT PA-X alone or by the NatA-modified PA-X E2A mutants expressed together with each of the PR8 proteins PB2, PB1, PA, HA, NP, NA, M1, M2, NS1, and NEP (data not shown). For the PA segment, we used a version with a mutation in the frameshift sequence that reduces PA-X production. When NS1 was co-transfected with PA-X E2A, there was an increase in host shutoff activity (Fig. 6). In contrast, co-expression of other PR8 proteins had no effect (data not shown). This result suggests that during infection, there is a functional interaction between PA-X and NS1 that promotes the host shutoff activity of PA-X, although PA-X can technically function in the absence of additional influenza proteins.

Discussion

Taken together, our results reveal that N-terminal acetylation of PA-X supports host shutoff activity in two separate ways: it is required for nuclear localization of PA-X as well as a second yet undetermined process that promotes PA-X activity. Interestingly, the two processes have slightly different requirements for the modification. Addition of the acetyl group at either the first residue, i.e. the initiator methionine, or the second residue following initiator methionine excision

promotes nuclear localization of PA-X. However, mutants that are modified at the second residue like PA-X E2A do not downregulate RNAs, despite being localized to the nucleus. Therefore, the acetyl group on the initiator methionine is specifically required for the full host shutoff activity of PA-X, at least when this protein is expressed ectopically. Interestingly, during infection, we found that the retained methionine is not required for the host shutoff activity of PA-X. This restoration of host shutoff activity during infection is due, at least in part, to the viral protein NS1.

This is the first time that a role for the N-terminal region of PA-X in nuclear localization has been reported. Previous studies have identified regions in the C-terminal X-ORF of PA-X for nuclear localization. Here we show that those regions alone are not enough for the nuclear localization of PA-X, as none of these regions were mutated in our studies. Conversely, N-terminal acetylation of PA-X is also not enough to direct PA-X nuclear localization, because the N-terminal domain of PA-X alone does not traffic to the nucleus[3,33,34] even though it should be N-terminally acetylated by NatB. The full structure of PA-X has not yet been solved, and further work needs to be done to determine how the acetylated N-terminus and the C-terminal X-ORF work together to drive the nuclear localization of PA-X.

While N-terminal acetylation has been previously linked to protein localization[28–31,42], this function has generally been confined to membrane localization. This is the first report of regulation of nuclear localization by this modification. For membrane localization, N-terminal acetylation directs proteins to membranes through two mechanisms: protein-protein interactions with integral membrane proteins[29,30] and direct interactions with membranes[42]. It is possible that the N-terminal acetylation stabilizes the PA-X N terminus, increasing binding affinity between PA-X and interacting proteins that mediate nuclear localization. While the details of this effect are still unknown, these results suggest that N-terminal acetylation has a broader range of

functions in protein localization than previously reported and mediates interactions with additional trafficking proteins.

How N-terminal acetylation separately mediates the nuclear localization and the host shutoff activity of PA-X remains unclear. Previous studies on N-terminal acetylation have shown that this modification impacts protein-protein interactions[22–25]. Biochemically, N-terminal acetylation eliminates the N-terminal positive charge of the first amino acid and increases hydrophobicity. This may allow for a new protein interaction surface that is unavailable when the N-terminus is unmodified. For example, the N-terminal acetylated initiator methionine of the NEDD8-conjugating E2 enzyme Ubc12 allows for docking in the hydrophobic pocket of the co-E3 ligase Dcn1, thus promoting the function of the E2/E3 complex[22,23]. The structure of the interaction interfaces may also be subtly different depending on whether the initiator methionine is retained. In the case of PA-X, general N-terminal acetylation may support interactions with a cytoplasmic protein that is involved in the nuclear import of PA-X, but retention of a modified methionine may be needed for an interaction that allows PA-X to reach and/or degrade its RNA targets in the nucleus. Alternatively, it is possible that while the N-terminally acetylated E2A-modified mutants enter the nucleus, they are not able to localize to the correct subnuclear compartment to downregulate host mRNAs. These possibilities should be addressed in future studies.

Another open question is how NS1 promotes PA-X host shutoff activity. In addition to our results, a recent study by Bougon et al. supports this idea, as they found some NS1 mutations abolished host shutoff in PR8-infected cells[35]. Our results show that PA-X and NS1 do not simply have an additive effect on RNA downregulation, as PR8 NS1 has no effect on RNA levels on its own, as previously reported[43]. NS1 binds many host factors[44–50], in some cases causing these proteins to relocalize from nuclear speckles to the nucleoplasm[46]. Thus, it is possible that the relocalization of a host protein promotes the host shutoff activity of PA-X by

facilitating protein-protein interactions in the correct nuclear compartment. It is also possible that NS1 stabilizes these protein interactions in some way. Alternatively, NS1 may promote PA-X host shutoff by preventing host mRNA export from the nucleus. Efficient export of mature mRNAs is coupled to their synthesis by RNA polymerase II and additional processing events. In some strains of influenza A virus, NS1 prevents RNA maturation by binding the poly(A) tail and preventing mRNA export from the nucleus to the cytoplasm[51]. Our lab has reported that PA-X preferentially downregulates spliced mRNAs that are synthesized by RNA polymerase II[3,5,52]. Thus, it is possible that PA-X targets are retained in the nucleus by NS1, allowing for an increase in mRNA degradation. In addition, we have also shown that PA-X preferentially cleaves GCUG tetramers located in single-stranded regions of hairpin loops. As NS1 binds double-stranded RNA[53,54], it could stabilize the hairpin region of PA-X targets, allowing for easier substrate targeting by PA-X.

While NS1 restores part of PA-X function, it does not explain the whole difference between ectopic expression and infection. Because influenza A virus infection alters the levels of some host proteins[55,56], this change may lead to an increase in PA-X host shutoff activity. In particular, proteins that are associated with protein binding, localization, and transport are upregulated in influenza A virus-infected human lung cells[55]. A possible model is that modification of PA-X at the second residue following methionine excision in the NatA-acetylated PA-X E2A mutant results in decreased PA-X binding affinity for an interacting protein compared to initiation methionine acetylation. However, during infection, this interacting protein is upregulated, and there is a consequent improvement in its binding to PA-X E2A. This increase, alongside the effects that were seen with NS1, could explain the restoration of activity seen during infection. In general, both NS1-dependent and NS1-independent effects of infection on PA-X activity will need to be defined in the future.

Overall, we have discovered that N-terminal acetylation functionally promotes the host shutoff activity of PA-X by separately influencing PA-X subcellular localization and the overall ability of PA-X to downregulate its targets. Our results suggest that the initiator methionine specifically promotes RNA downregulation. In the future, it will be important to determine how N-terminal acetylation contributes to structural differences or PA-X interactions with other proteins and PA-X substrates. Additionally, in the context of cellular biology, these studies contribute new evidence that N-terminal acetylation supports the correct subcellular localization of modified proteins. To our knowledge, this is also the first time that N-terminal acetylation has been shown to promote nuclear localization. Indeed, our studies highlight that N-terminal acetylation is multifaceted in its regulations of modified proteins and that this modification remains incompletely understood.

Materials and Methods

Plasmids

pCR3.1-PA-X-myc, pCR3.1-PA-X D108A-myc, pCR3.1-PA-X-eGFP, pCR3.1-PA-X D108A-eGFP, pCR3.1-PB2-myc, pCR3.1-PB1-myc, pCR3.1-PA(fs)-myc, pCR3.1-HA-myc, pCR3.1-NP-myc, pCR3.1 NA-myc, pCR3.1-M1-myc, pCR3.1-NS1-myc, and pCR3.1-NEP-myc from the PR8 strain were gifts from C. McCormick (Dalhousie University, Halifax, NS, Canada) and generated as previously described[57]. pCDNA3.1-eGFP was a gift from B. Glaunsinger (University of California, Berkley, Berkley, CA, USA). The luciferase construct with the β-globin intron was a gift from G. Dreyfuss (University of Pennsylvania, Philadelphia, PA, USA)[58]. The rescue plasmids encoding the 8 segments of PR8 virus (pHW191-PB2 to pHW198-NS) were gifts from R. Webby (St. Jude Children's Research Hospital, Memphis, TN, USA)[59]. Gibson cloning using HiFi assembly mix (New England Biolabs) was used to make pCR3.1-PA-X-NLS-eGFP by

amplifying the PR8 sequence of PA-X from pCR3.1-PA-X-myc and the eGFP sequence from pCDNA3.1-eGFP. The nuclear localization sequence (NLS) in pCR3.1-PA-X-NLS-eGFP was designed into the primers for Gibson cloning. Similar PA-X-eGFP fusion constructs were made using the PA-Xs from A/Perth/16/2009 H3N2 (Perth) and A/Tennessee/1-560/09 H1N1 (H1N1pdm09). The E2 mutations in the pCR3.1-PA-X-eGFP constructs with PA-Xs from PR8, Perth, and H1N1pdm09 were generated using the QuikChange II site-directed mutagenesis kit (Agilent). The PR8 pHW-PA(ΔX) plasmid was generated as previously described[5,52] from pHW193 by introducing mutations that reduce frameshifting events and add a premature stop codon in the PA-X reading frame, but that are silent in the PA reading frame.

Cell lines and transfections

Human embryonic kidney (HEK) 293T cells and Madin-Darby canine kidney (MDCK) cells were commercially obtained from ATCC (CRL-3216 and CCL-34, respectively). Both cell lines were maintained in high glucose Dulbecco's modified Eagle's medium (DMEM) supplemented with 10% fetal bovine serum at 37ºC in 5% CO2 atmosphere. To measure host shutoff activity of PA-X or the PA-X E2 mutants, HEK293T cells were plated on 24-well plates and transfected with 500 ng total DNA (including 25 ng PA-X constructs and 50 ng pCMV luciferase + intron construct) in 10% FBS in DMEM using jetPRIME transfection reagent (Polyplus). Cells were collected 24 hours post-transfection for RNA extraction and purification. To determine subcellular localization of PA-X, HEK293T cells were transfected as described above and plated onto poly-L-lysine (Sigma) treated glass coverslips. 24 hours post-transfection, cells were fixed with 4% paraformaldehyde and prepared for confocal microscopy. To measure the host shutoff activity of PA-X during influenza A virus infections, HEK293Ts were plated in 24-well plates that were pre-treated with 10 ug/ml fibronectin, 100 ug/ml BSA, and 30 ug/ml bovine collagen in modified Eagle's medium (MEM). FIbronectin, BSA and bovine collagen were UV crosslinked on the plate for 30 minutes before addition of the cells. This treatment was done to increase

HEK293T adhesion to the plate during the procedure. Cells were then transfected with 500 ng total DNA in infection media (0.5% low-endotoxin bovine serum albumin (BSA) in high glucose DMEM) using jetPRIME transfection reagent (Polyplus). 8 hours post-transfection, media was removed and cells were mock infected or infected with WT PR8 or PR8 PA(ΔX). 24 hours post-transfection/16 hours post-infection, cells were collected for RNA extraction and purification.

Viruses and infections

Wild-type influenza A virus A/Puerto Rico/9/1934 H1N1 (PR8) and the mutant recombinant virus PR8 PA(ΔX) were generated using the 8-plasmid reverse genetic system[59] as previously described[3,5,52]. Viral stocks were produced in MDCK cells and infectious titers were determined by plaque assays in MDCK cells using 1.2% Avicel overlays[60]. Briefly, confluent MDCK cells were infected with low volumes of tenfold serially diluted virus stocks in triplicate for 1 hour. Cells were then washed twice with PBS before the addition of overlay media (1.2% Avicel, 1X MEM, 0.5% low-endotoxin BSA in DMEM, and 1 ug/ml TPCK-treated trypsin) and incubated for 4 days at 37ºC in 5% CO_2 atmosphere. After 4 days, cells were fixed with 4% paraformaldehyde and stained with crystal violet to observe plaques. Influenza A virus infections following HEK293T transfections were performed in infection media (0.5% low-endotoxin BSA in high glucose DMEM). Briefly, transfected HEK293T cells were mock-infected or infected with WT PR8 or PR8 PA(ΔX) in infection media supplemented with 0.5 ug/ml TPCK-treated trypsin at a multiplicity of infection (MOI) of 1 for 16 hours at 37ºC in 5% CO_2 atmosphere. Cells were then collected and lysed in RNA lysis buffer for RNA isolation.

RNA purification, cDNA preparation and qPCR

RNA was extracted and purified using the Quick-RNA miniprep kit (Zymo Research) following the manufacturer's protocol. Purified RNA was treated with Turbo DNase (Life Technologies), then reverse transcribed using iScript supermix (Bio-Rad) per manufacturer's protocol. qPCR

was performed using iTaq Universal SYBR Green Supermix (Bio-Rad) on the Bio-Rad CFX Connect Real-Time PCR Detection System or CFX Duet Real-Time PCR System and analyzed with Bio-Rad CFX Manager software or Bio-Rad CFX Maestro software, respectively. Primers used for the qPCR were:

Primer name	**Primer sequence (5' → 3')**
18S forward	GTAACCCGTTGAACCCCATT
18S reverse	CCATCCAATCGGTAGTAGCG
Luciferase forward	ATCGAGGTGGACATTACCTACG
Luciferase reverse	CGCTCGTTGTAGATGTCGTTAG
G6PD forward	TGAGCCAGATAGGCTGGAA
G6PD reverse	TAACGCAGGCGATGTTGTC
PR8 HA forward	CTGGACCTTGCTAAAACCCG
PR8 HA reverse	TCTGGAAAGGGAGACTGCTG

Confocal microscopy

HEK293T cells were grown on glass coverslips pretreated with poly-L-lysine, which were prepared following the manufacturer's protocol (Sigma-Aldrich). 24 hours after cells were transfected with eGFP-tagged PA-X variants as outlined above, cells were washed twice with PBS and fixed with 4% paraformaldehyde. Cells were permeabilized in 0.1% Triton X100 and nuclei were stained with 1:10,000 dilution of Hoechst 3342 Fluorescent Stain (Fisher Scientific). Coverslips were then mounted on glass slides using ProLong Gold Antifade Mountant (Thermo Fisher). Images were taken with the Nikon A1R Confocal Microscope or the Leica Stellaris Confocal Microscope. To determine colocalization between the eGFP-tagged PA-X proteins and the nucleus, quantification of fluorescence overlap between eGFP and the nuclear stain was

done on at least 10 random eGFP-positive cells using Just Another Colocalization Program (JACoP) in ImageJ[37].

Quantification and Statistical Analysis

Data are plotted as the mean +/- standard error of the mean and represent three or more independent biological replicates. Statistical analyses were performed using GraphPad Prism (v10.0.2. For multiple comparisons, one-way analysis of variance (ANOVA) with Dunnett's multiple comparison test or two-way ANOVA with uncorrected Fisher's LSD multiple comparison test were used and significance was defined as <0.05. Where indicated, levels of significance are denoted as follows: *P < 0.05, **P < 0.01, ***P < 0.001.

Acknowledgements

We thank Drs C. McCormick, D. Khaperskyy, B. Glaunsinger, G. Dreyfuss, and R. Webby for constructs. We thank Drs C. McCormick, D. Khaperskyy and members of the Gaglia laboratory for feedback and advice. Support for this research was provided by NIH grant R01AI137358 (to MMG), a Rosenberg fellowship from Tufts Graduate School of Biomedical Sciences (to RD) and by the University of Wisconsin-Madison, Office of the Vice Chancellor for Research and Graduate Education with funding from the Wisconsin Alumni Research Foundation.

References

1. Chaimayo, C., Dunagan, M., Hayashi, T., Santoso, N. & Takimoto, T. Specificity and functional interplay between influenza virus PA-X and NS1 shutoff activity. *PLOS Pathog.* **14**, e1007465 (2018).
2. Jagger, B. W. *et al.* An Overlapping Protein-Coding Region in Influenza A Virus Segment 3 Modulates the Host Response. *Science* **337**, 199–204 (2012).

3. Khaperskyy, D. A., Schmaling, S., Larkins-Ford, J., McCormick, C. & Gaglia, M. M. Selective Degradation of Host RNA Polymerase II Transcripts by Influenza A Virus PA-X Host Shutoff Protein. *PLoS Pathog.* **12**, (2016).

4. Hayashi, T., MacDonald, L. A. & Takimoto, T. Influenza A Virus Protein PA-X Contributes to Viral Growth and Suppression of the Host Antiviral and Immune Responses. *J. Virol.* **89**, 6442–6452 (2015).

5. Gaucherand, L. *et al.* The Influenza A Virus Endoribonuclease PA-X Usurps Host mRNA Processing Machinery to Limit Host Gene Expression. *Cell Rep.* **27**, 776-792.e7 (2019).

6. Oishi, K., Yamayoshi, S., Kozuka-Hata, H., Oyama, M. & Kawaoka, Y. N-Terminal Acetylation by NatB Is Required for the Shutoff Activity of Influenza A Virus PA-X. *Cell Rep.* **24**, 851–860 (2018).

7. Brown, J. L. & Roberts, W. K. Evidence that approximately eighty per cent of the soluble proteins from Ehrlich ascites cells are Nalpha-acetylated. *J. Biol. Chem.* **251**, 1009–1014 (1976).

8. Arnesen, T. *et al.* Proteomics analyses reveal the evolutionary conservation and divergence of N-terminal acetyltransferases from yeast and humans. *Proc. Natl. Acad. Sci. U. S. A.* **106**, 8157–8162 (2009).

9. Aksnes, H., Drazic, A., Marie, M. & Arnesen, T. First Things First: Vital Protein Marks by N-Terminal Acetyltransferases. *Trends Biochem. Sci.* **41**, 746–760 (2016).

10. Aksnes, H. *et al.* An Organellar Nα-Acetyltransferase, Naa60, Acetylates Cytosolic N Termini of Transmembrane Proteins and Maintains Golgi Integrity. *Cell Rep.* **10**, 1362–1374 (2015).

11. Starheim, K. K., Gevaert, K. & Arnesen, T. Protein N-terminal acetyltransferases: when the start matters. *Trends Biochem. Sci.* **37**, 152–161 (2012).

12. Ree, R., Varland, S. & Arnesen, T. Spotlight on protein N-terminal acetylation. *Exp. Mol. Med.* **50**, 90 (2018).

13. Arnesen, T. Towards a Functional Understanding of Protein N-Terminal Acetylation. *PLOS Biol.* **9**, e1001074 (2011).
14. Myklebust, L. M. *et al.* Biochemical and cellular analysis of Ogden syndrome reveals downstream Nt-acetylation defects. *Hum. Mol. Genet.* **24**, 1956–1976 (2015).
15. Hwang, C.-S., Shemorry, A. & Varshavsky, A. N-Terminal Acetylation of Cellular Proteins Creates Specific Degradation Signals. *Science* **327**, 973–977 (2010).
16. Shemorry, A., Hwang, C.-S. & Varshavsky, A. Control of protein quality and stoichiometries by N-terminal acetylation and the N-end rule pathway. *Mol. Cell* **50**, 540–551 (2013).
17. Xu, F. *et al.* Two N-Terminal Acetyltransferases Antagonistically Regulate the Stability of a Nod-Like Receptor in Arabidopsis. *Plant Cell* **27**, 1547–1562 (2015).
18. Sheikh, T. I., de Paz, A. M., Akhtar, S., Ausió, J. & Vincent, J. B. MeCP2_E1 N-terminal modifications affect its degradation rate and are disrupted by the Ala2Val Rett mutation. *Hum. Mol. Genet.* **26**, 4132–4141 (2017).
19. Holmes, W. M., Mannakee, B. K., Gutenkunst, R. N. & Serio, T. R. Loss of amino-terminal acetylation suppresses a prion phenotype by modulating global protein folding. *Nat. Commun.* **5**, 4383 (2014).
20. Trexler, A. J. & Rhoades, E. N-terminal acetylation is critical for forming α-helical oligomer of α-synuclein. *Protein Sci. Publ. Protein Soc.* **21**, 601–605 (2012).
21. Bartels, T., Choi, J. G. & Selkoe, D. J. α-Synuclein occurs physiologically as a helically folded tetramer that resists aggregation. *Nature* **477**, 107–110 (2011).
22. Scott, D. C., Monda, J. K., Bennett, E. J., Harper, J. W. & Schulman, B. A. N-Terminal Acetylation Acts as an Avidity Enhancer Within an Interconnected Multiprotein Complex. *Science* **334**, 674–678 (2011).
23. Monda, J. K. *et al.* Structural Conservation of Distinctive N-terminal Acetylation-Dependent Interactions across a Family of Mammalian NEDD8 Ligation Enzymes. *Structure* **21**, 42–53 (2013).

24. Yang, D. *et al.* Nα-acetylated Sir3 stabilizes the conformation of a nucleosome-binding loop in the BAH domain. *Nat. Struct. Mol. Biol.* **20**, 1116–1118 (2013).

25. Arnaudo, N. *et al.* The N-terminal acetylation of Sir3 stabilizes its binding to the nucleosome core particle. *Nat. Struct. Mol. Biol.* **20**, 1119–1121 (2013).

26. Singer, J. M. & Shaw, J. M. Mdm20 protein functions with Nat3 protein to acetylate Tpm1 protein and regulate tropomyosin–actin interactions in budding yeast. *Proc. Natl. Acad. Sci. U. S. A.* **100**, 7644–7649 (2003).

27. Coulton, A. T., East, D. A., Galinska-Rakoczy, A., Lehman, W. & Mulvihill, D. P. The recruitment of acetylated and unacetylated tropomyosin to distinct actin polymers permits the discrete regulation of specific myosins in fission yeast. *J. Cell Sci.* **123**, 3235–3243 (2010).

28. Forte, G. M. A., Pool, M. R. & Stirling, C. J. N-Terminal Acetylation Inhibits Protein Targeting to the Endoplasmic Reticulum. *PLOS Biol.* **9**, e1001073 (2011).

29. Setty, S. R. G., Strochlic, T. I., Tong, A. H. Y., Boone, C. & Burd, C. G. Golgi targeting of ARF-like GTPase Arl3p requires its Nα-acetylation and the integral membrane protein Sys1p. *Nat. Cell Biol.* **6**, 414–419 (2004).

30. Behnia, R., Panic, B., Whyte, J. R. C. & Munro, S. Targeting of the Arf-like GTPase Arl3p to the Golgi requires N-terminal acetylation and the membrane protein Sys1p. *Nat. Cell Biol.* **6**, 405–413 (2004).

31. Behnia, R., Barr, F. A., Flanagan, J. J., Barlowe, C. & Munro, S. The yeast orthologue of GRASP65 forms a complex with a coiled-coil protein that contributes to ER to Golgi traffic. *J. Cell Biol.* **176**, 255–261 (2007).

32. Shi, M. *et al.* Evolutionary Conservation of the PA-X Open Reading Frame in Segment 3 of Influenza A Virus. *J. Virol.* **86**, 12411–12413 (2012).

33. Oishi, K., Yamayoshi, S. & Kawaoka, Y. Mapping of a Region of the PA-X Protein of Influenza A Virus That Is Important for Its Shutoff Activity. *J. Virol.* **89**, 8661–8665 (2015).

506 34. Hayashi, T., Chaimayo, C., McGuinness, J. & Takimoto, T. Critical Role of the PA-X C-
507 Terminal Domain of Influenza A Virus in Its Subcellular Localization and Shutoff Activity. *J.*
508 *Virol.* **90**, 7131–7141 (2016).
509 35. Bougon, J. *et al.* Influenza A virus NS1 effector domain is required for PA-X mediated host
510 shutoff. 2023.10.02.560421 Preprint at https://doi.org/10.1101/2023.10.02.560421 (2023).
511 36. Goetze, S. *et al.* Identification and Functional Characterization of N-Terminally Acetylated
512 Proteins in Drosophila melanogaster. *PLOS Biol.* **7**, e1000236 (2009).
513 37. Bolte, S. & Cordelières, F. P. A guided tour into subcellular colocalization analysis in light
514 microscopy. *J. Microsc.* **224**, 213–232 (2006).
515 38. Adam, S. A., Lobl, T. J., Mitchell, M. A. & Gerace, L. Identification of specific binding
516 proteins for a nuclear location sequence. *Nature* **337**, 276–279 (1989).
517 39. Wingfield, P. N-Terminal Methionine Processing. *Curr. Protoc. Protein Sci.* **88**, 6.14.1-6.14.3
518 (2017).
519 40. Van Damme, P. Charting the N-Terminal Acetylome: A Comprehensive Map of Human NatA
520 Substrates. *Int. J. Mol. Sci.* **22**, 10692 (2021).
521 41. CDC. Weekly U.S. Influenza Surveillance Report. *Centers for Disease Control and*
522 *Prevention* https://www.cdc.gov/flu/weekly/index.htm (2023).
523 42. Dikiy, I. & Eliezer, D. N-terminal acetylation stabilizes N-terminal helicity in lipid- and micelle-
524 bound α-synuclein and increases its affinity for physiological membranes. *J. Biol. Chem.*
525 **289**, 3652–3665 (2014).
526 43. Salvatore, M. *et al.* Effects of Influenza A Virus NS1 Protein on Protein Expression: the NS1
527 Protein Enhances Translation and Is Not Required for Shutoff of Host Protein Synthesis. *J.*
528 *Virol.* **76**, 1206–1212 (2002).
529 44. Koliopoulos, M. G. *et al.* Molecular mechanism of influenza A NS1-mediated TRIM25
530 recognition and inhibition. *Nat. Commun.* **9**, 1820 (2018).

45. Hale, B. G., Jackson, D., Chen, Y.-H., Lamb, R. A. & Randall, R. E. Influenza A virus NS1 protein binds p85β and activates phosphatidylinositol-3-kinase signaling. *Proc. Natl. Acad. Sci. U. S. A.* **103**, 14194–14199 (2006).

46. Chen, Z., Li, Y. & Krug, R. M. Influenza A virus NS1 protein targets poly(A)-binding protein II of the cellular 3'-end processing machinery. *EMBO J.* **18**, 2273–2283 (1999).

47. Das, K. *et al.* Structural basis for suppression of a host antiviral response by influenza A virus. *Proc. Natl. Acad. Sci. U. S. A.* **105**, 13093–13098 (2008).

48. Chien, C. *et al.* Biophysical Characterization of the Complex between Double-Stranded RNA and the N-Terminal Domain of the NS1 Protein from Influenza A Virus: Evidence for a Novel RNA-Binding Mode. *Biochemistry* **43**, 1950–1962 (2004).

49. Burgui, I., Aragón, T., Ortín, J. & Nieto, A. PABP1 and eIF4GI associate with influenza virus NS1 protein in viral mRNA translation initiation complexes. *J. Gen. Virol.* **84**, 3263–3274 (2003).

50. Aragón, T. *et al.* Eukaryotic Translation Initiation Factor 4GI Is a Cellular Target for NS1 Protein, a Translational Activator of Influenza Virus. *Mol. Cell. Biol.* **20**, 6259–6268 (2000).

51. Qiu, Y. & Krug, R. M. The influenza virus NS1 protein is a poly(A)-binding protein that inhibits nuclear export of mRNAs containing poly(A). *J. Virol.* **68**, 2425–2432 (1994).

52. Gaucherand, L., Iyer, A., Gilabert, I., Rycroft, C. H. & Gaglia, M. M. Cut site preference allows influenza A virus PA-X to discriminate between host and viral mRNAs. *Nat. Microbiol.* **8**, 1304–1317 (2023).

53. Min, J.-Y. & Krug, R. M. The primary function of RNA binding by the influenza A virus NS1 protein in infected cells: Inhibiting the 2′-5′ oligo (A) synthetase/RNase L pathway. *Proc. Natl. Acad. Sci. U. S. A.* **103**, 7100–7105 (2006).

54. Lu, Y., Qian, X. Y. & Krug, R. M. The influenza virus NS1 protein: a novel inhibitor of pre-mRNA splicing. *Genes Dev.* **8**, 1817–1828 (1994).

55. Coombs, K. M. *et al.* Quantitative Proteomic Analyses of Influenza Virus-Infected Cultured Human Lung Cells. *J. Virol.* **84**, 10888–10906 (2010).

56. Haas, K. M. *et al.* Proteomic and genetic analyses of influenza A viruses identify pan-viral host targets. *Nat. Commun.* **14**, 6030 (2023).

57. Khaperskyy, D. A. *et al.* Influenza A Virus Host Shutoff Disables Antiviral Stress-Induced Translation Arrest. *PLoS Pathog.* **10**, e1004217 (2014).

58. Younis, I. *et al.* Rapid-Response Splicing Reporter Screens Identify Differential Regulators of Constitutive and Alternative Splicing. *Mol. Cell. Biol.* **30**, 1718–1728 (2010).

59. Hoffmann, E., Krauss, S., Perez, D., Webby, R. & Webster, R. G. Eight-plasmid system for rapid generation of influenza virus vaccines. *Vaccine* **20**, 3165–3170 (2002).

60. Matrosovich, M., Matrosovich, T., Garten, W. & Klenk, H.-D. New low-viscosity overlay medium for viral plaque assays. *Virol. J.* **3**, 63 (2006).

Figure legends

Fig. 1 N-terminal acetylation of PA-X is required for nuclear localization. A) Diagram showing which Nat complexes acetylate nascent proteins depending on the first two amino acids. WT PA-X and the PA-X E2 mutants E2D and E2N are modified by NatB (purple), PA-X E2L and E2M mutants are modified by NatC (yellow), and PA-X E2A, E2S, and E2V mutants are modified by NatA (blue). The PA-X E2P mutant should be unmodified. B-G) HEK293T cells were transfected for 24 hours with empty vector, WT PR8 PA-X-eGFP, the catalytically inactive PA-X D108A-eGFP mutant, or the indicated PR8 PA-X-eGFP mutants carrying changes in the second amino acid. For B, a PR8 PA-X E2P mutant carrying an SV40 nuclear localization sequence (PA-X E2P-NLS-eGFP) was also transfected. B,E) mRNA levels of a co-transfected luciferase reporter were measured by RT-qPCR and normalized to 18S rRNA. Levels are plotted as change relative to vector transfected cells. C,F) Confocal microscopy was used to image eGFP-positive cells. Nuclei are stained with Hoechst. Representative images are shown. D,G) Manders' overlap coefficients for colocalization of nuclei and GFP signal on images were determined using JACoP in ImageJ. Each data point represents 10-15 eGFP positive cells. Manders' overlap coefficient values represent the following localization: ~1: all protein is nuclear; ~0.5: protein is diffuse throughout the cell.
Error bars indicate the standard error of the mean. (n>3) *p < 0.05 **p < 0.01 ***p < 0.001 ****p < 0.0001 ANOVA with Dunnett's multiple comparison test compared to wild-type PA-X.

Fig. 2 General N-terminal acetylation is sufficient for PA-X localization to the nucleus. HEK293T cells were transfected for 24 hours with empty vector, WT PR8 PA-X-eGFP, the catalytically inactive PA-X D108A-eGFP mutant, or the indicated NatA-modified PR8 PA-X-eGFP mutants carrying changes in the second amino acid. A) mRNA levels of a co-transfected luciferase reporter were measured by RT-qPCR and normalized to 18S rRNA. Levels are plotted as change relative to vector transfected cells. B) Confocal microscopy was used to

image eGFP, PA-X-eGFP (PA-X), PA-X E2A-eGFP (E2A), PA-X E2S-eGFP (E2S), and PA-X E2V-eGFP (E2V). Nuclei were stained with Hoechst. Representative images are shown. C) Manders' overlap coefficients for colocalization of nuclei and eGFP signal were determined on images using JACoP in ImageJ, where each point represents 10-15 eGFP-positive cells. Manders' overlap coefficient values represent the following localization: ~1: all protein is nuclear; ~0.5: protein is diffuse throughout the cell.
Error bars indicate the standard error of the mean. (n>3) *p < 0.05 **p < 0.01 ***p < 0.001 ****p < 0.0001 ANOVA with Dunnett's multiple comparison test compared to wild-type PA-X.

Fig. 3 N-terminal acetylation at the initiator methionine promotes PA-X host shutoff activity. HEK293T cells were transfected for 24 hours with empty vector, WT PR8 PA-X-eGFP, the catalytically inactive PA-X D108A-eGFP mutant, or the indicated NatC-modified PR8 PA-X-eGFP mutants carrying changes in the second amino acid. A) mRNA levels of a co-transfected luciferase reporter were measured by RT-qPCR and normalized to 18S rRNA. Levels are plotted as change relative to vector transfected cells. B) Confocal microscopy was used to image eGFP, PA-X-eGFP (PA-X), PA-X E2M-eGFP (E2M), and PA-X E2L-eGFP (E2L). Nuclei were stained with Hoechst. Representative images are shown. C) Manders' overlap coefficients for colocalization of nuclei and eGFP signal were determined on images using JACoP in ImageJ, where each point represents 10-15 eGFP-positive cells. Manders' overlap coefficient values represent the following localization: ~1: all protein is nuclear; ~0.5: protein is diffuse throughout the cell.
Error bars indicate the standard error of the mean. (n>3) *p < 0.05 **p < 0.01 ***p < 0.001 ****p < 0.0001 ANOVA with Dunnett's multiple comparison test compared to wild-type PA-X.

Fig. 4 N-terminal acetylation also regulates the activity of PA-X proteins from circulating influenza A virus subtypes. HEK293T cells were transfected for 24 hours with empty vector,

622 WT PR8 PA-X-eGFP, WT H1N1pdm09 PA-X-eGFP, or WT Perth PA-X-eGFP or the indicated
623 PR8 PA-X-eGFP mutants carrying changes in the second amino acid. mRNA levels of a co-
624 transfected luciferase reporter were measured by RT-qPCR and normalized to 18S rRNA.
625 Levels are plotted as change relative to vector transfected cells. Error bars indicate the standard
626 error of the mean. (n>3) *p < 0.05 **p < 0.01 ***p < 0.001 ****p < 0.0001 ANOVA with Dunnett's
627 multiple comparison test compared to wild-type PA-X.
628
629 **Fig. 5 During infection, N-terminal acetylation of PA-X at any position is sufficient for**
630 **host shutoff activity.** HEK293T cells were transfected for 24 hours with empty vector, eGFP,
631 and eGFP-tagged WT PA-X, or the following eGFP-tagged mutants: unmodified mutant PA-X
632 E2P (gray), NatB-modified PA-X E2D mutant (purple), NatA-modified mutant E2A (blue), or
633 NatC-modified mutant E2M (yellow). Eight hours post-transfection, cells were mock infected or
634 infected with WT PR8 or the PA-X deficient PR8 PA(ΔX) virus at an MOI of 1. RNA samples
635 were collected 16 hrs post-infection (24 hrs post-transfection). mRNA levels of A) viral HA
636 mRNA, B) endogenous G6PD mRNA, and C) the co-transfected luciferase reporter were
637 measured by RT-qPCR and normalized to 18S rRNA. For B,C, Levels are plotted as change
638 relative to vector transfected cells. For C, significance is calculated in comparison to the WT
639 transfected conditions in each infection condition. (n>3) *p < 0.05 **p < 0.01 ***p < 0.001 ****p <
640 0.0001 Ordinary two-way ANOVA with uncorrected Fisher's LSD multiple comparison test
641 compared to the wild-type PA-X in each infection condition.
642
643 **Fig. 6 Influenza A virus protein NS1 potentiates PA-X activity.** A) HEK293T cells were
644 transfected for 24 hours with empty vector, WT PA-X-eGFP, the NatA-modified mutant PA-X
645 E2A-eGFP, myc-tagged PR8 NS1 or a combination of these constructs. mRNA levels of a co-
646 transfected luciferase reporter were measured by RT-qPCR and normalized to 18S rRNA.

Levels are plotted as change relative to vector transfected cells. (n>3) *p < 0.05 ANOVA with Dunnett's multiple comparison test compared to wild-type PA-X.

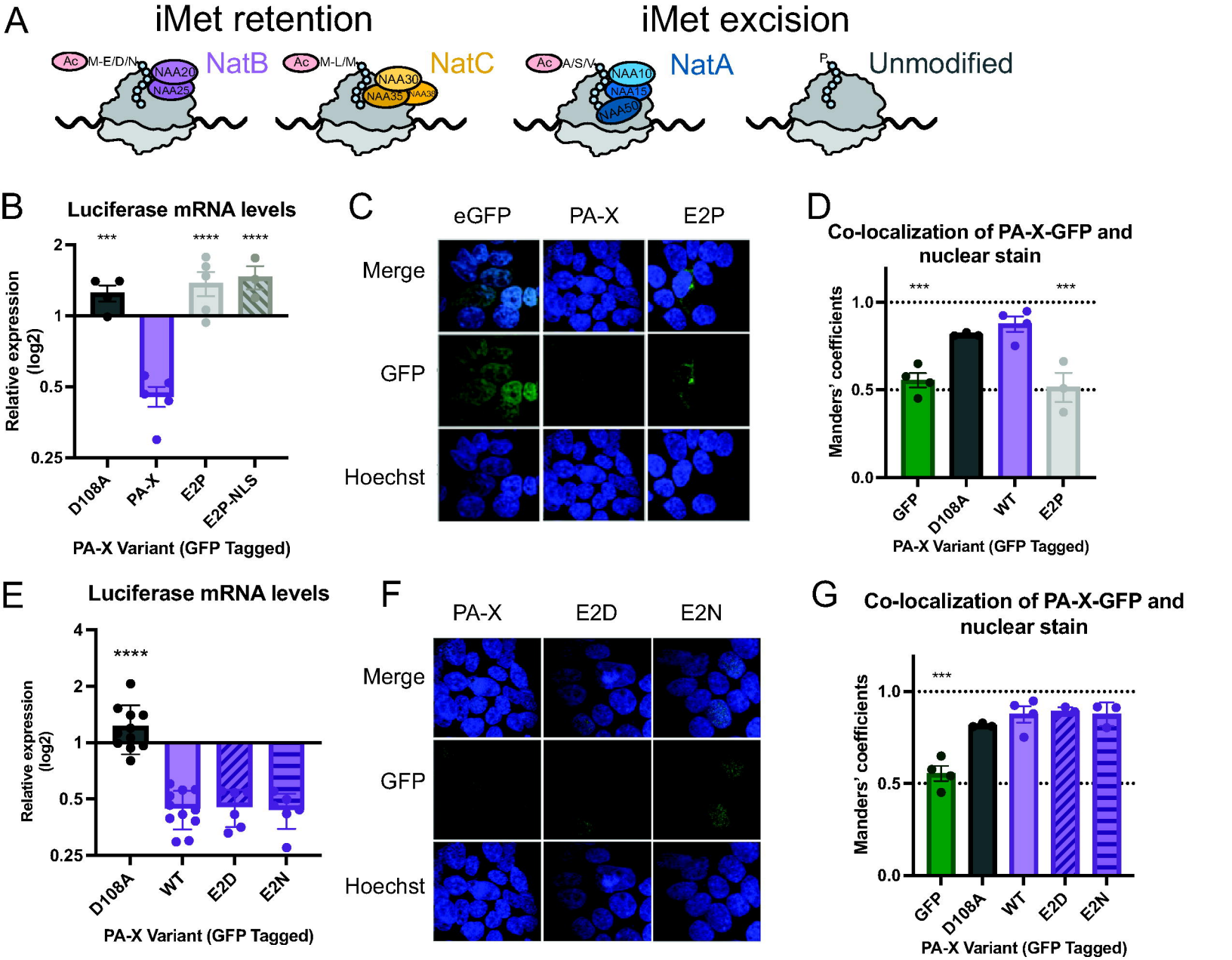

Fig. 1 N-terminal acetylation of PA-X is required for nuclear localization. A) Diagram showing which Nat complexes acetylate nascent proteins depending on the first two amino acids. WT PA-X and the PA-X E2 mutants E2D and E2N are modified by NatB (purple), PA-X E2L and E2M mutants are modified by NatC (yellow), and PA-X E2A, E2S, and E2V mutants are modified by NatA (blue). The PA-X E2P mutant should be unmodified. B-G) HEK293T cells were transfected for 24 hours with empty vector, WT PR8 PA-X-eGFP, the catalytically inactive PA-X D108A-eGFP mutant, or the indicated PR8 PA-X-eGFP mutants carrying changes in the second amino acid. For B, a PR8 PA-X E2P mutant carrying an SV40 nuclear localization sequence (PA-X E2P-NLS-eGFP) was also transfected. B,E) mRNA levels of a co-transfected luciferase reporter were measured by RT-qPCR and normalized to 18S rRNA. Levels are plotted as change relative to vector transfected cells. C,F) Confocal microscopy was used to image eGFP-positive cells. Nuclei are stained with Hoechst. Representative images are shown. D,G) Manders' overlap coefficients for colocalization of nuclei and GFP signal on images were determined using JACoP in ImageJ. Each data point represents 10-15 eGFP positive cells. Manders' overlap coefficient values represent the following localization: ~1: all protein is nuclear; ~0.5: protein is diffuse throughout the cell.

Error bars indicate the standard error of the mean. (n>3) *p < 0.05 **p < 0.01 ***p < 0.001 ****p < 0.0001 ANOVA with Dunnett's multiple comparison test compared to wild-type PA-X.

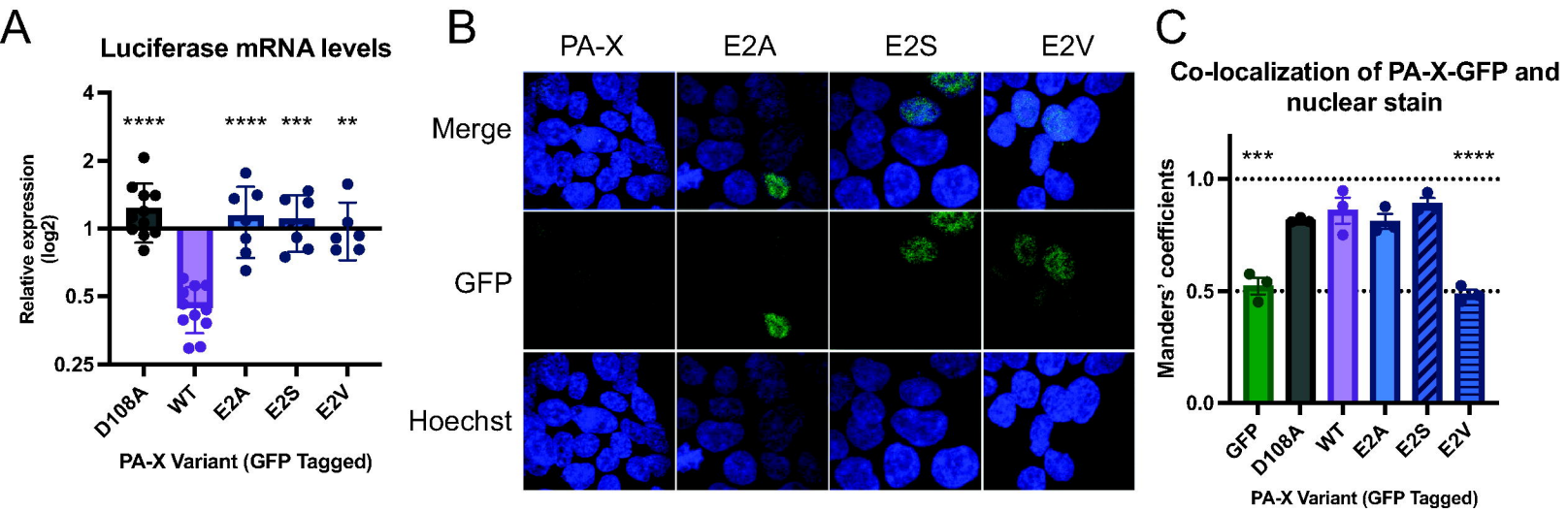

Fig. 2 General N-terminal acetylation is sufficient for PA-X localization to the nucleus. HEK293T cells were transfected for 24 hours with empty vector, WT PR8 PA-X-eGFP, the catalytically inactive PA-X D108A-eGFP mutant, or the indicated NatA-modified PR8 PA-X-eGFP mutants carrying changes in the second amino acid. A) mRNA levels of a co-transfected luciferase reporter were measured by RT-qPCR and normalized to 18S rRNA. Levels are plotted as change relative to vector transfected cells. B) Confocal microscopy was used to image eGFP, PA-X-eGFP (PA-X), PA-X E2A-eGFP (E2A), PA-X E2S-eGFP (E2S), and PA-X E2V-eGFP (E2V). Nuclei were stained with Hoechst. Representative images are shown. C) Manders' overlap coefficients for colocalization of nuclei and eGFP signal were determined on images using JACoP in ImageJ, where each point represents 10-15 eGFP-positive cells. Manders' overlap coefficient values represent the following localization: ~1: all protein is nuclear; ~0.5: protein is diffuse throughout the cell.

Error bars indicate the standard error of the mean. (n>3) *p < 0.05 **p < 0.01 ***p < 0.001 ****p < 0.0001 ANOVA with Dunnett's multiple comparison test compared to wild-type PA-X.

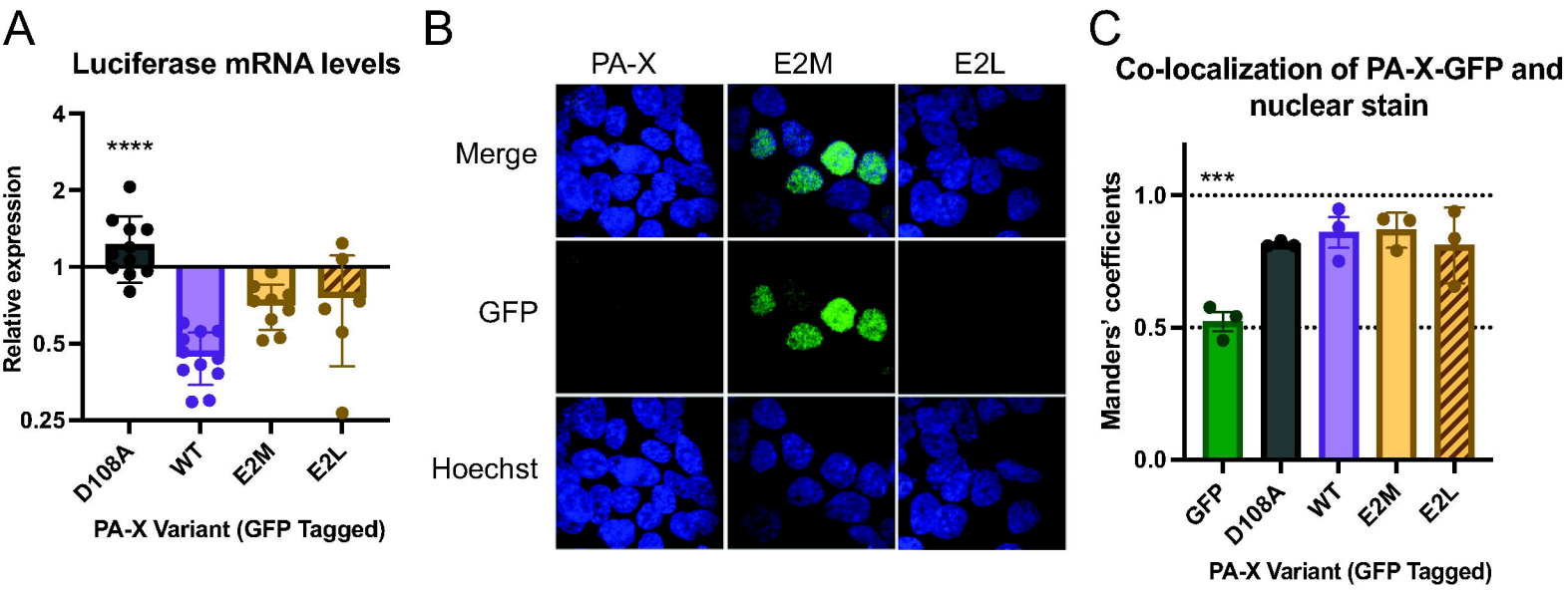

Fig. 3 N-terminal acetylation at the initiator methionine promotes PA-X host shutoff activity. HEK293T cells were transfected for 24 hours with empty vector, WT PR8 PA-X-eGFP, the catalytically inactive PA-X D108A-eGFP mutant, or the indicated NatC-modified PR8 PA-X-eGFP mutants carrying changes in the second amino acid. A) mRNA levels of a co-transfected luciferase reporter were measured by RT-qPCR and normalized to 18S rRNA. Levels are plotted as change relative to vector transfected cells. B) Confocal microscopy was used to image eGFP, PA-X-eGFP (PA-X), PA-X E2M-eGFP (E2M), and PA-X E2L-eGFP (E2L). Nuclei were stained with Hoechst. Representative images are shown. C) Manders' overlap coefficients for colocalization of nuclei and eGFP signal were determined on images using JACoP in ImageJ, where each point represents 10-15 eGFP-positive cells. Manders' overlap coefficient values represent the following localization: ~1: all protein is nuclear; ~0.5: protein is diffuse throughout the cell.
Error bars indicate the standard error of the mean. (n>3) *p < 0.05 **p < 0.01 ***p < 0.001 ****p < 0.0001 ANOVA with Dunnett's multiple comparison test compared to wild-type PA-X.

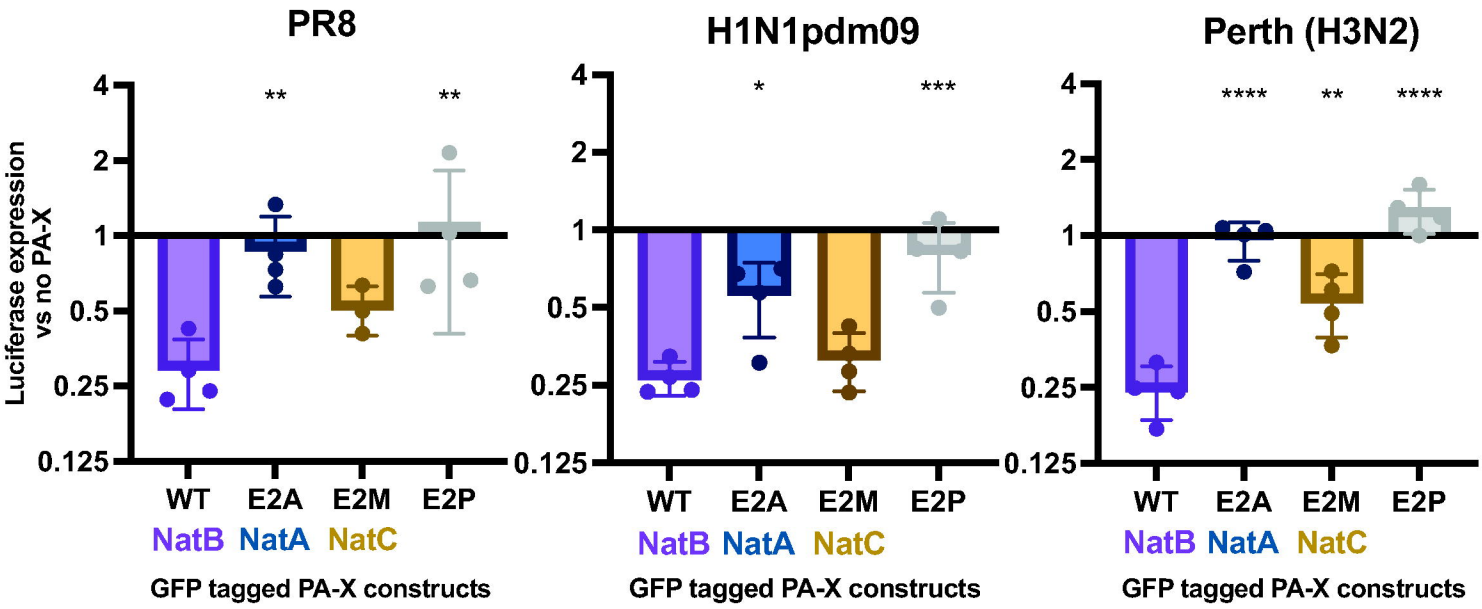

Fig. 4 N-terminal acetylation also regulates the activity of PA-X proteins from circulating influenza A virus subtypes. HEK293T cells were transfected for 24 hours with empty vector, WT PR8 PA-X-eGFP, WT H1N1pdm09 PA-X-eGFP, or WT Perth PA-X-eGFP or the indicated PR8 PA-X-eGFP mutants carrying changes in the second amino acid. mRNA levels of a co-transfected luciferase reporter were measured by RT-qPCR and normalized to 18S rRNA. Levels are plotted as change relative to vector transfected cells. Error bars indicate the standard error of the mean. (n>3) *p < 0.05 **p < 0.01 ***p < 0.001 ****p < 0.0001 ANOVA with Dunnett's multiple comparison test compared to wild-type PA-X.

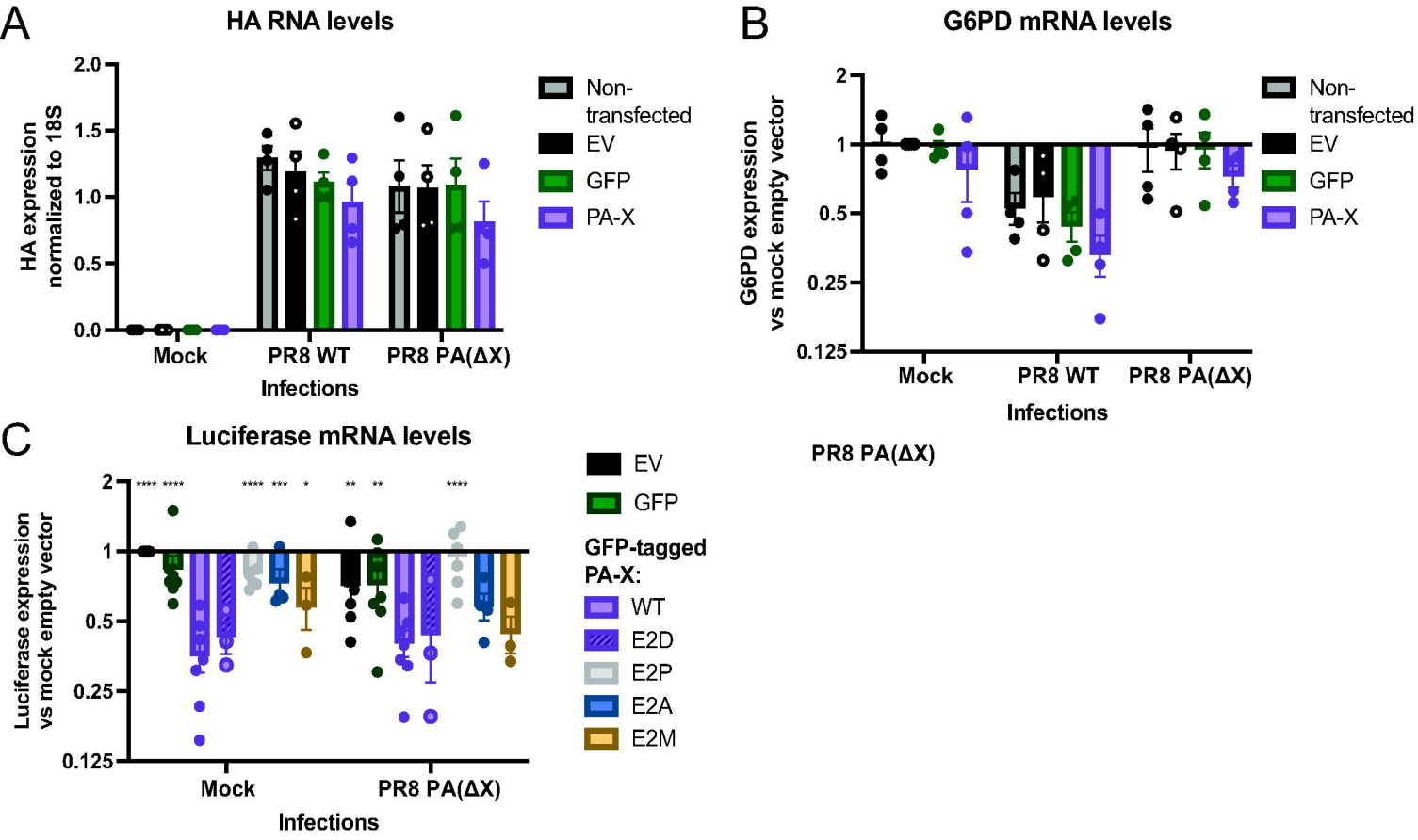

Fig. 5 During infection, N-terminal acetylation of PA-X at any position is sufficient for host shutoff activity. HEK293T cells were transfected for 24 hours with empty vector, eGFP, and eGFP-tagged WT PA-X, or the following eGFP-tagged mutants: unmodified mutant PA-X E2P (gray), NatB-modified PA-X E2D mutant (purple), NatA-modified mutant E2A (blue), or NatC-modified mutant E2M (yellow). Eight hours post-transfection, cells were mock infected or infected with WT PR8 or the PA-X deficient PR8 PA(ΔX) virus at an MOI of 1. RNA samples were collected 16 hrs post-infection (24 hrs post-transfection). mRNA levels of A) viral HA mRNA, B) endogenous G6PD mRNA, and C) the co-transfected luciferase reporter were measured by RT-qPCR and normalized to 18S rRNA. For B,C, Levels are plotted as change relative to vector transfected cells. For C, significance is calculated in comparison to the WT transfected conditions in each infection condition. (n>3) *p < 0.05 **p < 0.01 ***p < 0.001 ****p < 0.0001 Ordinary two-way ANOVA with uncorrected Fisher's LSD multiple comparison test compared to the wild-type PA-X in each infection condition.

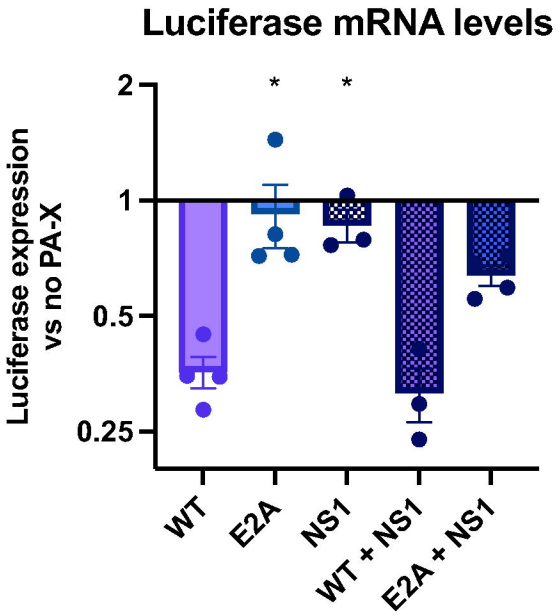

Fig. 6 Influenza A virus protein NS1 potentiates PA-X activity. A) HEK-293T cells were transfected for 24 hours with empty vector, WT PA-X-eGFP, the NatA-modified mutant PA-X E2A-eGFP, myc-tagged PR8 NS1 or a combination of these constructs. mRNA levels of a co-transfected luciferase reporter were measured by RT-qPCR and normalized to 18S rRNA. Levels are plotted as change relative to vector transfected cells. (n>3) *p < 0.05 ANOVA with Dunnett's multiple comparison test compared to wild-type PA-X.